Polymer 50 (2009) 825–831

Contents lists available at ScienceDirect

Polymer

journal homepage: www.elsevier.com/locate/polymer

Fabrication of an asymmetric hollow particle with a thermo-sensitive PNIPAM inside corona

Zhe Li, De'an Xiong, Bing Xu, Chenglin Wu, Yingli An, Rujiang Ma, Linqi Shi*

Key Laboratory of Functional Polymer Materials, Ministry of Education, Institute of Polymer Chemistry, Nankai University, Tianjin 300071, China

ARTICLE INFO

Article history:
Received 20 August 2008
Received in revised form
11 November 2008
Accepted 2 December 2008
Available online 9 December 2008

Keywords:
Asymmetric hollow particle
Cross-linked shell
Self-assembly

ABSTRACT

Asymmetric hollow particles were fabricated from the self-assembly of block copolymers poly(N-isopropylacrylamide)-*block*-poly(4-vinylpyridine) (PNIPAM-*b*-P4VP) and poly(ethylene glycol)-*block*-poly(acrylic acid) (PEG-*b*-PAA) in water. The shell of the asymmetric hollow particle was a polyion complex layer which acted as a semipermeable membrane. Outside the shell were PEG hydrophilic layers and inside were thermo-sensitive PNIPAM chains. When temperature was higher than the lower critical solution temperature (LCST) of PNIPAM, it became insoluble and collapsed onto the shrinking shell to form a hydrophobic lumen. The whole process was characterized by dynamic light scattering (DLS), static light scattering (SLS), transmission electron microscopy (TEM), atom force microscopy (AFM) and nuclear magnetic resonance (NMR).

1. Introduction

Hollow particle or vesicle, which consisted of a hollow interior surrounded by a thin wall and formed from the self-assembly of block copolymers, has been the focus of intensive studies in recent years [1–5]. From the first reports on the spontaneous formation of defined morphologies in (aqueous) dispersion by the self-assembly of block copolymers [6,7] until present studies, it has been suggested that this cell-like structure possesses the potential of application in drug delivery systems and artificial cells [8]. Great efforts were paid for the improvement of hollow particles or vesicles. Jiang et al. developed an approach to prepare vesicles which was simple without chemical bonds connecting and avoided costly and time-consuming synthesis of block copolymers [9]. They also succeeded in obtaining micelles and hollow nanospheres by a "block-copolymer-free strategy" [10,11]. Weda et al. have reported the preparation of the hollow particles with larger interiors which could encapsulate large compounds, such as proteins and DNA molecules [12]. Kataoka et al. prepared a novel entity of a polymer vesicle by a simple mixing of a pair of oppositely charged block copolymers [13]. Meier and coworkers have prepared Poly(2-methyloxazoline)-*b*-poly(dimethylsiloxane)-*b*-poly(2-methyloxazoline) (PMOXA-*b*-PDMS-*b*-PMOXA) vesicle which had a structure with hydrophilic chains on both sides of the PDMS shell in aqueous solution [14]. The hydrophilic blocks from both the outer and the inner surfaces of the hydrophobic shell enhanced the stability of hollow particles.

Further works have also been reported from Meier that a new vesicle having asymmetric, membrane-like superstructure was fabricated by the self-assembly of the amphiphilic PEO–PDMS–PMOXA triblock copolymer in aqueous media. In the vesicle the longer of the two hydrophilic segments PEO or PMOXA was toward the outside. This asymmetric vesicle had a particular structure which imitated most membrane proteins: different hydrophilic blocks tethered to the outside and inside of the shell [15]. Similarly, Eisenberg and Luo synthesized an asymmetric vesicle by dissolving PAA-*b*-PS-*b*-P4VP triblock copolymers in an acidic aqueous solution [16]. The same vesicles with asymmetric structure were also fabricated by directly mixing the PS-*b*-PAA and PS-*b*-P4VP diblock in aqueous solution [17].

Hollow particles or vesicles used as drug carriers, that is loading and releasing of hydrophilic drugs from hollow particles have been exploited since a decade ago [18]. Usually, most of drugs were hydrophilic and loaded by diffusion after the fabrication of the hollow particles [19]. Ahmed et al. fabricated a vesicle with the vesicular lumen for a hydrophilic drug doxorubicin and the thick wall for a hydrophobic drug paclitaxel. Similar work was also reported that paclitaxel could self-assemble into thicker hydrophobic bilayers [20], which was just like the hydrophobic drug partitions into the micelle core [21]. However, it did not show the advantage of hollow particles that is they could load molecules in its lumen. Besides, the shells of the hollow particles mentioned

* Corresponding author. Tel.: +86 22 23506103; fax: +86 22 23503510.
E-mail address: shilinqi@nankai.edu.cn (L. Shi).

0032-3861/$ – see front matter © 2008 Elsevier Ltd. All rights reserved.
doi:10.1016/j.polymer.2008.12.004

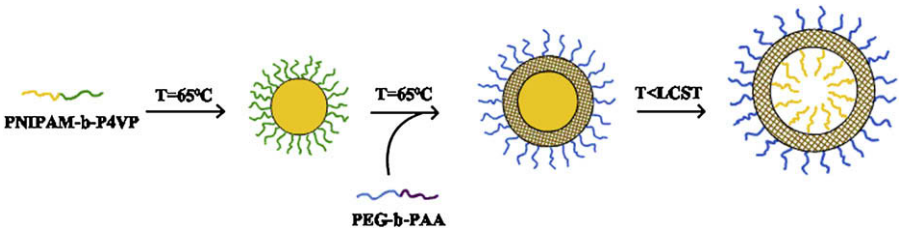

Scheme 1. Formation of asymmetric hollow particles with complex CLS and phase transition PNIPAM inside corona.

above formed from the insoluble polymer chains, and this continuous hydrophobic phase layer resulted in the lack of permeability and blocked the small molecules to pass through [22,23]. In fact, this situation could be easily changed by a semipermeable membrane which is prepared through the simple mixing of a pair of oppositely charged block copolymers in an aqueous medium [13].

Herein, we propose a strategy to prepare asymmetric hollow particle with a hydrophilic PNIPAM inside corona, a cross-linked P4VP/PAA shell, and a hydrophilic PEG corona. When temperature went above the LCST again, the PNIPAM block would collapse onto the cross-linked shell (CLS) gradually and another asymmetric structure formed with hydrophilic block outside and hydrophobic block inside the shell. It is possible for this hydrophobic lumen to encapsulate the hydrophobic drugs. Besides, the CLS could act as a semipermeable membrane and the permeability of the CLS can be controlled by the cross-linking density. The fabrication process is shown in Scheme 1.

2. Experimental section

2.1. Materials

Polyethylene glycol monomethyl ether (CH_3O–PEG_{114}–OH) ($M_n = 5000$ and the polydispersity index PDI = 1.05) was purchased from Fluka. N-Isopropylacrylamide (NIPAM, Acros Organics, 99%) was recrystallized from an n-hexane/benzene mixture and dried under vacuum prior to use. 4-Vinylpyridine (4VP) and tert-butyl acrylate (tBA) were purchased from Aldrich and purified by vacuum distillation before use. CuCl was purchased from Aldrich and purified according to Ref. [24]. Tris[2-(dimethylamino)-ethyl]amine (Me_6TREN) was synthesized according to Ref. [25]. All water used in this study was purified with a Millipore Mill-Q system, and the resistivity was above 16 MΩ cm. Other reagents were used as-received.

2.2. Synthesis of PNIPAM–Cl macroinitiator and $PNIPAM_{53}$-b-$P4VP_{109}$

$PNIPAM_{53}$-*b*-$P4VP_{109}$ was synthesized by atom transfer radical polymerization (ATRP) according to our previous work [26]. The details are explained below: PNIPAM–Cl was synthesized by ATRP of N-isopropylacrylamide using methyl 2-chlorpropionate as the initiator and CuCl/Me_6TREN as the catalyst system. 0.200 g of CuCl and 0.460 g of Me_6TREN were added into the reaction flask, followed by adding 5.00 mL of toluene. Subsequently, 5.00 g of N-isopropylacrylamide and 0.081 g of methyl 2-chlorpropionate were added into the flask and degassed with nitrogen. After freeze–degas–thaw cycles, polymerization was performed at 40 °C for 24 h and the product PNIPAM–Cl was purified by passing through an Al_2O_3 column to remove the copper catalyst followed by precipitation in iced diethyl ether. The precipitate of PNIPAM–Cl was then filtered under vacuum and dried in a vacuum oven at room temperature. The PNIPAM-*b*-P4VP was synthesized by ATRP using PNIPAM–Cl as macroinitiator. The polymerization procedure was similar to that described above, except that the solvent used in this polymerization was a mixture of isopropyl alcohol and 2-butanone (8:2 by volume).

2.3. Synthesis of PEG_{114}-b-$PtBA_{156}$

PEG_{114}-*b*-PtBA was synthesized by ATRP using PEG–Br as macroinitiator and the procedure is described as follows: The synthesis of PEG–Br macroinitiator was presented in Ref. [27]. 2.0 g of PEO_{114}–Br, 0.04 g of CuBr and 0.07 g of N,N,N′,N′,N-pentamethyldiethylenetriamine (PMDETA) were added to a reaction flask then followed by addition of 6 mL of mixed solution of butanone and 2-propanol (8:2 by volume). The solution was stirred and then 5.0 g of tBA was added into the flask. The reaction mixture underwent three times of freeze–degas–thaw cycles and flame-sealed under vacuum. Polymerization was performed at 110 °C for 8 h. The solution was dissolved in CH_2Cl_2 followed by passing through an Al_2O_3 column to remove the copper catalyst. The solution was then condensed by rotary evaporation and poured into 10-fold excess of water. The precipitate of PEO_{114}-*b*-$PtBA_{156}$ was filtered under vacuum and dried in a vacuum oven at room temperature to obtain a canary solid.

2.4. Preparation of PEG_{114}-b-PAA

The block copolymer PEG_{114}-*b*-$PtBA_{156}$ was dissolved in dichloromethane and a 10-fold molar excess trifluoroacetatic acid (TFA) (with respect to the tert-butyl group) was added. This solution mixture was then vigorously stirred at room temperature for a week. The resulting PEG_{114}-*b*-PAA was precipitated out from the reaction mixture by n-hexane three times. They were filtered, washed with dichloromethane, and dried under vacuum to constant weight.

2.5. Preparation of asymmetric hollow particle

The block copolymer $PNIPAM_{53}$-*b*-$P4VP_{109}$ was first dissolved in de-ionized water at pH = 4.5 to make a stock polymer solution with a concentration of 0.15 mg mL^{-1}. Then PEG_{114}-*b*-PAA_{156} solutions with four concentrations 0.1, 0.05, 0.02 and 0.01 mg mL^{-1} were prepared in the same de-ionized water at pH = 4.5 (as shown in Table 1). Subsequently, the $PNIPAM_{53}$-*b*-$P4VP_{109}$ solution was kept in water bath of 65 °C overnight. Then equal volume of prepared PEG_{114}-*b*-PAA_{156} solutions with different concentrations was added under vigorous stirring. The solutions were stored at 65 °C for at least 3 days to make sure the completeness of the interaction

Table 1
Different concentrations of the four samples.

	Sample 1	Sample 2	Sample 3	Sample 4
PEG_{114}-*b*-PAA_{156}/mg mL^{-1}	0.10	0.05	0.02	0.01
$PNIPAM_{53}$-*b*-$P4VP_{109}$/mg mL^{-1}	0.15	0.15	0.15	0.15
Weight ratio	2:3	1:3	2:15	1:15
Unit ratio of PAA/P4VP	1:1	1:2	1:5	1:10

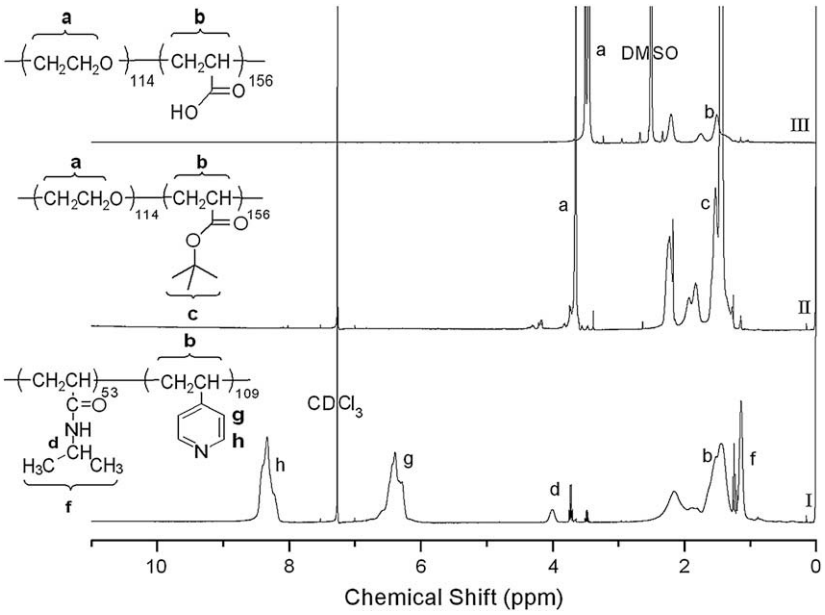

Fig. 1. ^{1}H NMR spectra of PNIPAM$_{53}$-*b*-P4VP$_{109}$ in $CDCl_3$ (I), and PEG$_{114}$-*b*-PtBA$_{156}$ before (in $CDCl_3$) (II) and after (PEG$_{114}$-*b*-PAA$_{156}$, in DMSO-d_6) hydrolysis (III).

between P4VP and PAA blocks. The solutions then were stored at 4 °C overnight and then at room temperature (25 °C) for another 3 days. When PNIPAM block became fully stretched, the anticipant asymmetric hollow particle formed.

2.6. Characterization

The ^{1}H NMR spectra were recorded using a Varian UNITY-plus 400 spectrometer and chemical shifts were given in ppm relative to TMS. GPC was performed on a Waters 600E gel permeation chromatography analysis system, $CHCl_3$ and THF were used as eluents and narrowly distributed polystyrene was used as calibration standard. Dynamic Light Scattering (DLS) and Static Light Scattering (SLS) measurements were preformed on a laser light scattering spectrometer (BI-S200 M) with a digital correlator at 532 nm at a given temperature. All the samples were obtained by filtering through a 0.45 μm Millipore filter into a clean scintillation vial. The detailed procedure of LLS measurements can be found in Wu's paper [28]. Transmission Electron Microscopy (TEM) measurements were performed with a commercial Jeol 100cii electron microscope at an acceleration voltage of 100 kV. Atom Force Microscopy (AFM) images were collected on a Digital Instruments Nanoscope IV multimode atomic force microscope (Veeco Metrology Group) in tapping mode.

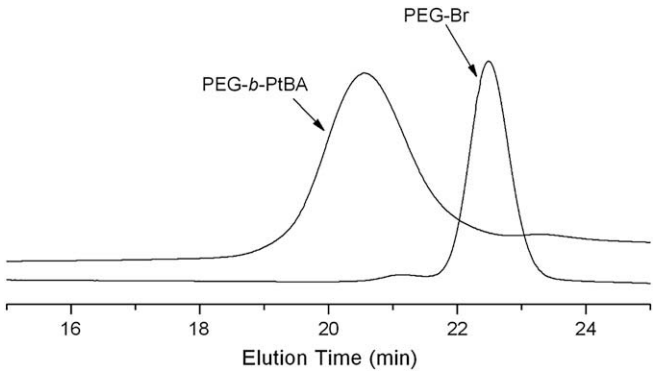

Fig. 2. The GPC results of PEG–Br and PEG-*b*-PtBA.

3. Results and discussions

The number-average molecular weight M_n of PNIPAM-*b*-P4VP measured by ^{1}H NMR and the polydispersity indices (PDIs) measured by GPC using $CHCl_3$ as the eluent were 1.62×10^4 g mol^{-1} and 1.26, respectively. The ^{1}H NMR spectra are shown in Fig. 1. The PDI of PEG-*b*-PtBA measured by GPC using THF as the eluent was 1.14, which is shown in Fig. 2. PEG-*b*-PAA was obtained by the hydrolysis of PEG-*b*-PtBA and its M_n measured by ^{1}H NMR was 1.63×10^4 g mol^{-1}.

The formation process of the asymmetric hollow particle underwent three stages: In the beginning at 65 °C, PNIPAM blocks in PNIPAM-*b*-P4VP unimers have already completed coil-to-globule phase transition and core–shell micelle with a PNIPAM core and a P4VP shell formed. Then, core–shell–corona micelle formed when PEG-*b*-PAA solution was added into PNIPAM-*b*-P4VP micellar

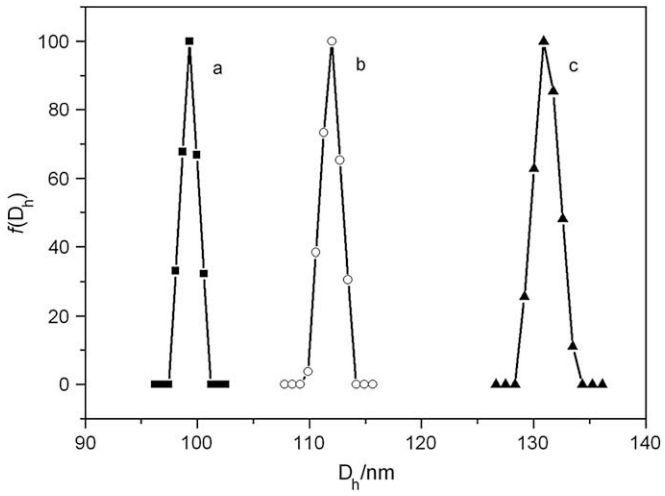

Fig. 3. The hydrodynamic diameter and distributions $f(D_h)$ of PNIPAM-*b*-P4VP micelle at 65 °C (a), CSC micelle formed when 0.10 mg mL^{-1} PEG-*b*-PAA water solution was added into equal volume of 0.15 mg mL^{-1} PNIPAM-*b*-P4VP water solution at 65 °C (b), and the formed swollen micelle at 25 °C (c). All DLS measurements were performed at a scattering angle of 90°.

Table 2
Summary of DLS and SLS results for CSC micelles and swollen micelles.

	R_g	R_h	R_g/R_h
CSC micelle	42.50	64.45	0.66
Swollen micelle	57.90	65.75	0.88

solution. Electrostatic interaction and hydrogen bonding were generated between P4VP and PAA blocks and resulted in interpolymer complexes [29]. Core–shell micelle turned into core–shell–corona micelle with a PNIPAM core, a P4VP/PAA complex shell and a PEG corona. Finally, when temperature was lower than LCST, the inner PNIPAM became hydrophilic and expanded in volume.

DLS measurements were employed to study the formation process of the asymmetric hollow particle (Fig. 3). At 65 °C, core–shell micelles with diameters of 99.0 nm were obtained (Fig. 3a). After the addition of PEG-*b*-PAA solution, the diameter increased to 112.0 nm (Fig. 3b), which indicated the formation of the P4VP/PAA complex shell. Finally at 25 °C, the particles with diameters of about 130.8 nm were collected which illustrated PNIPAM swelled (Fig. 3c).

It is well known that the ratio of gyration radius to hydrodynamic radius (R_g/R_h) reflects the morphology of particles dispersed in solution [30]. A smaller R_g/R_h value typically hints at a higher chain segment density. The DLS and SLS data are listed in Table 2. The R_g/R_h value of swollen micelle is 0.88, which is much larger than that of the CSC micelles (0.66), suggesting that PNIPAM became hydrophilic and swollen.

To observe the morphologies of this swollen micelle intuitively, the same sample was investigated with TEM after transferring the aqueous solutions to copper grid and removing the water at the same temperatures. It could be seen in Fig. 4A that the micelles with an average diameter of about 55.0 nm formed at 65 °C. Remarkable increase in the particle size from ca. 55.0 to ca. 75.0 nm, however, was observed when the TEM sample was prepared below LCST at 25 °C (Fig. 4B). The ca. 20 nm increment was caused by the swelling of PNIPAM core, which was consistent with the results of DLS measurements.

In Fig. 4B, the thickness of the swollen micelle walls could hardly be seen in the images. Besides, this is also a typical feature of soft (or rubber) hollow particles when observed under TEM. Due to the rubber-like wall, the deformed hollow particles have an almost constant thickness from the edge to the center and do not show any electron contrast, so the structure of this asymmetric hollow particle could not be viewed under TEM clearly [31]. Hence, AFM was employed to further observe the microstructures of the CSC micelles and swollen micelles.

The AFM images were taken from the same sample used in DLS and TEM with the Tapping mode. All the samples were prepared by the spin-coating process which is too fast to make samples restructure themselves during the drying process. The AFM images at 65 °C (A) and 25 °C (B) with surface profile curves are presented in Fig. 5. At 65 °C, PNIPAM block was hydrophobic and spherical micelles with a solid PNIPAM core formed. Fig. 5A shows the morphology of the core–shell micelles. At 25 °C, apparently, hollow particle structure existed according to the features of the surface curves (Fig. 5B). The average diameters of micelles at 65 °C and the hollow particles at 25 °C were ca. 62.6 nm and 82.2 nm, respectively. An AFM-tip broadening effect may exist [32], which led to the diameter larger than that of in TEM. Furthermore, the diameters of the micelles/hollow particles observed by TEM and AFM are smaller than the D_h measured by DLS, possibly because the micelles/hollow particles collapsed and shrank during the process of water evaporation [33].

The marked hollow particle in Fig. 5B was enlarged in 3D height image in Fig. 6. It is clear that the edge was higher than the center. Such features are observed since the center of the hollow particle is expected to be softer than the edge due to the existence of a hollow volume under the curved wall of the deformed hollow particle. The formation of the hollow volume was generated by the globule-to-coil phase transition of PNIPAM when the temperature was below LSCT, but the lumen formed in this way was relatively small.

In order to prove the formation of asymmetric particles, controlled two-dimensional Nuclear Overhauser Effect (2D NOE) Spectroscopy experiments were performed. 2D NOE is a two-dimensional NMR technique probing internuclear distances. When two protons of chemically different monomers are in close proximity (distance < 0.5 nm) cross peaks will present in the 2D ^{1}H NMR spectrum, due to the so-called Nuclear Overhauser Effect (NOE), which scales with r^{-6} (where r is the internuclear distance between the protons).

The sample was prepared by following the procedure in Section 2 and its contour plot of a 2D NOE experiment is presented in Fig. 7. Since in this asymmetric hollow particle, the PNIPAM and PEG blocks were separated by the P4VP/PAA complex shell (Scheme in

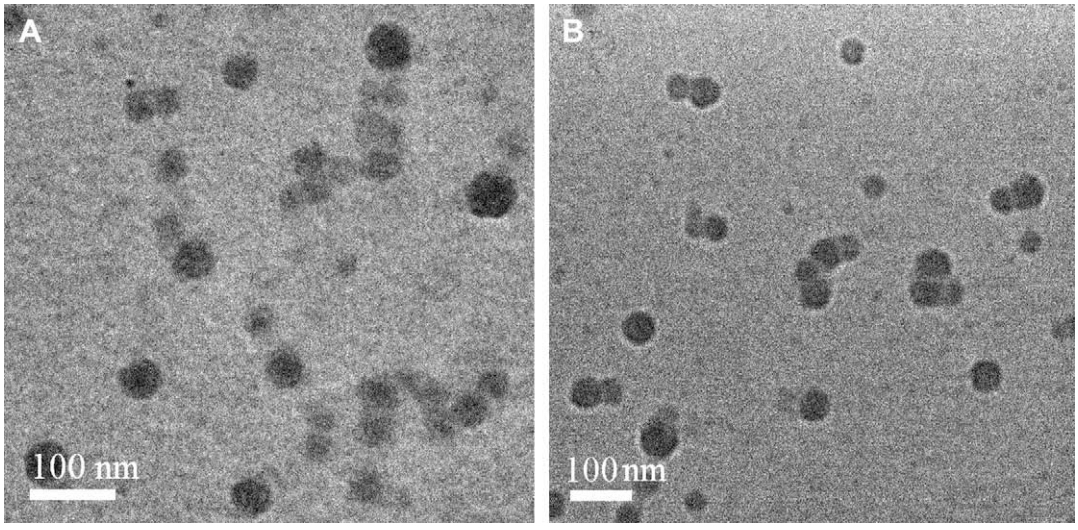

Fig. 4. TEM images of (A) CSC micelles at 65 °C (B) asymmetric hollow particles at 25 °C.

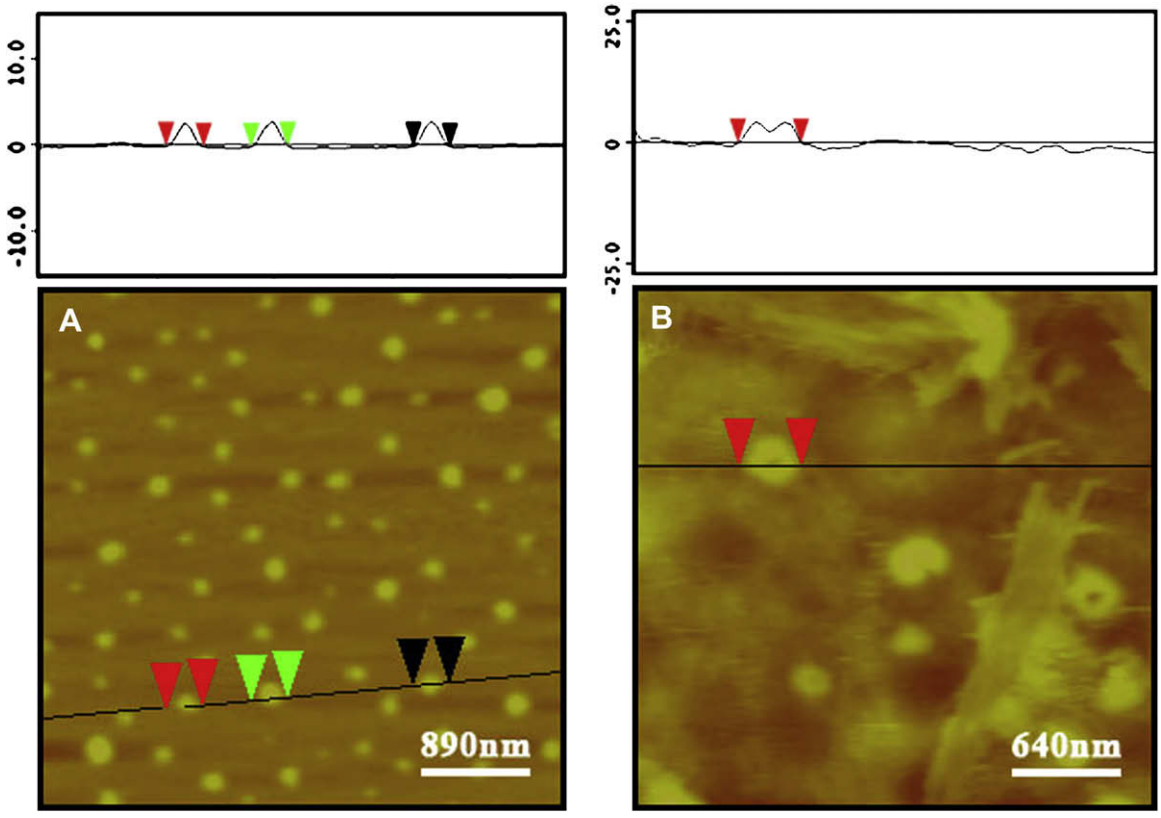

Fig. 5. Height images with the surface curves showing the features of the (A) micelles at 65 °C and (B) hollow asymmetric hollow particles at 25 °C.

Fig. 7), no cross peaks (arrows indicate positions where cross peaks should occur in case of close proximity) were observed [34] between the ^{1}H NMR signals of PEG (3.65 ppm) and PNIPAM (1.15 ppm (CH_3)). Comparative sample was prepared in another way by just adding PEG-*b*-PAA block dropwise into vigorously stirred PNIPAM-*b*-P4VP solution at room temperature. In this situation, the two block copolymers self-assembled into micelle structure with a P4VP/PAA complex core and PEG/PNIPAM coronas. Fig. 8 clearly shows cross peaks between corona blocks PEG and PNIPAM. This result indicated that the outside surface was composed of both PEG and PNIPAM chains, which was different from the asymmetric hollow particles. The 2D NOE experiments indicated no correlation between the protons in PEG and PNIPAM, validating the formation of asymmetric hollow particles.

As mentioned in Section 2, four samples with different weight ratios were prepared to examine the cross-linking density impact

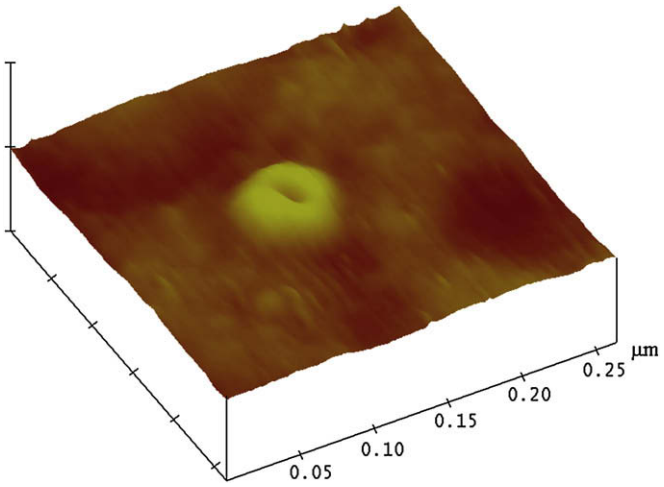

Fig. 6. 3D height image of the marked hollow particle.

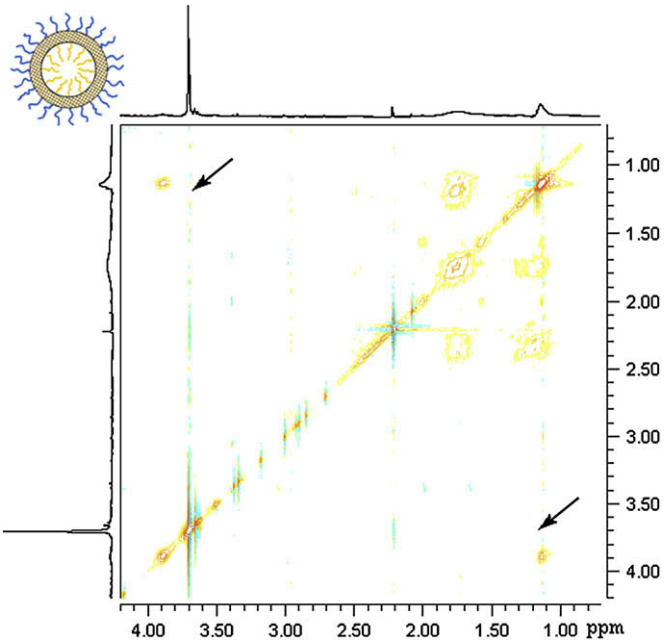

Fig. 7. 2D NOE contour plot of an asymmetric hollow particle. Arrows indicate where cross peaks between PNIPAM and PEO should occur in case of close proximity. The concentrations of PNIPAM-*b*-P4VP and PEG-*b*-PAA were 3 mg mL^{-1} and 2 mg mL^{-1}, respectively, keeping the weight ratio of PNIPAM-*b*-P4VP and PEG-*b*-PAA to be identical in Sample 1.

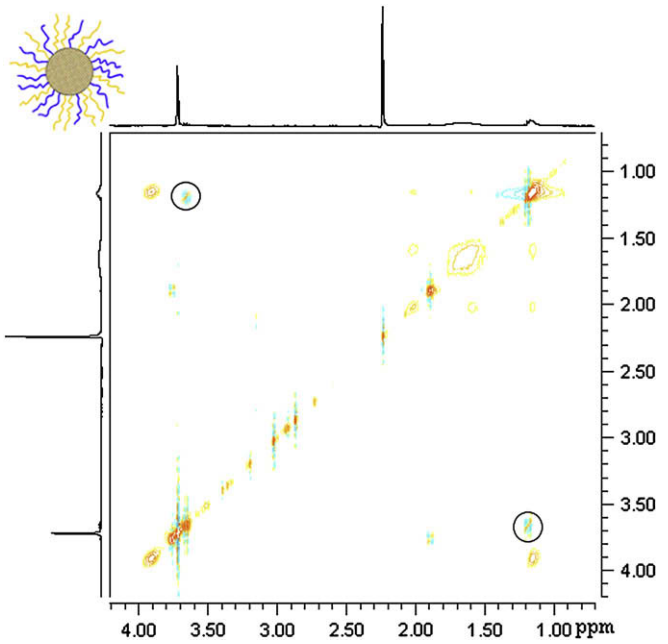

Fig. 8. 2D NOE contour plot of micelles self-assembled in room temperature. Circles indicate cross peaks between PNIPAM and PEG blocks.

on size of the asymmetric hollow particles. The hydrodynamic diameters and swelling ratios are listed in Table 3. Micelles with almost the same diameters were formed when PEG-*b*-PAA solution with different concentrations was added into an equal volume of PNIPAM-*b*-P4VP solution at 65 °C. When the weight ratio was 2/3, that is $PNIPAM_{53}$-*b*-$P4VP_{109}$ with 0.15 mg mL^{-1} and PEG_{114}-*b*-PAA_{156} with 0.10 mg mL^{-1} were mixed by equal volume, the number of P4VP units was almost the same as that of PAA units and the most dense cross-linked shell formed. PNIPAM core was tightly covered by the P4VP/PAA complex layer. In contrast, when $W_{PEG_{114}\text{-}b\text{-}PAA_{156}}/W_{PNIPAM_{53}\text{-}b\text{-}P4VP_{109}}$ ratios of the hollow particles were less than 2/3, the density of cross-linking was not as high as the completely complex ones and the shells were in a loose state, so their D_h were a little larger.

When the solution temperature was 25 °C, as mentioned before, the temperature-sensitive PNIPAM core became hydrophilic and swelled. However, the swelling ratio (V_{25}/V_{65}) of Sample 1 just reached 1.60. Obviously, the PNIPAM block was not fully stentering [29]. In the case of Sample 1, all the pyridyl units in P4VP interacted with carboxyls in PAA, which resulted in the highly cross-linked shell. Since a balance exists between the core expansion and the CLS restriction which was affected by the degree of shell cross-linking and would limit the expansion, the low swelling ratio of Sample 1 was due to highly cross-linked shell.

According to the explanation above, the swelling behavior of the hollow particles was highly dependent on the degree of cross-linking and can be tuned by the cross-linking density of the shell.

Table 3
Swelling ratios obtained from different cross-linking densities of the shells.

	$W_{PEG_{114}\text{-}b\text{-}PAA_{156}}/W_{PNIPAM_{53}\text{-}b\text{-}P4VP_{109}}$	Unit ratio of PAA/P4VP	D_h at 65 °C (nm)	D_h at 25 °C (nm)	Swelling ratio (V_{25}/V_{65})
Sample 1	2/3	ca. 1:1	112.0	130.8	1.6
Sample 2	1/3	ca. 1:2	113.4	149.7	2.3
Sample 3	2/15	ca. 1:5	114.3	199.5	5.3
Sample 4	1/15	ca. 1:10	118.7	266.2	11.2

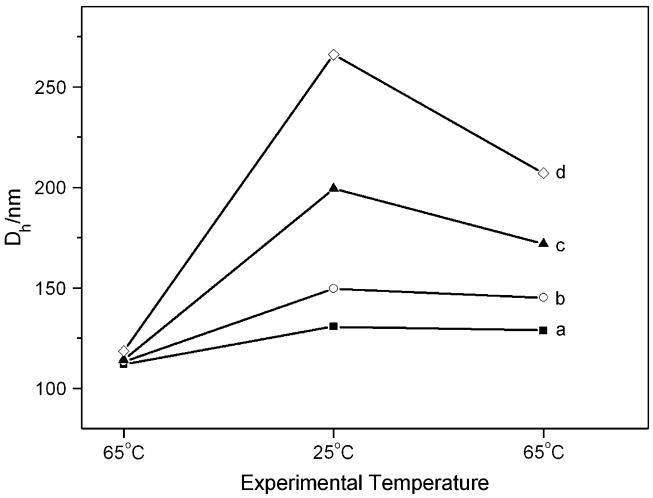

Fig. 9. The size changing of asymmetric hollow particles when different concentrations of PEG-*b*-PAA were added into 0.15 mg mL^{-1} PNIPAM-*b*-P4VP at different temperatures. (a) Sample 1 (b) Sample 2 (c) Sample 3 (d) Sample 4.

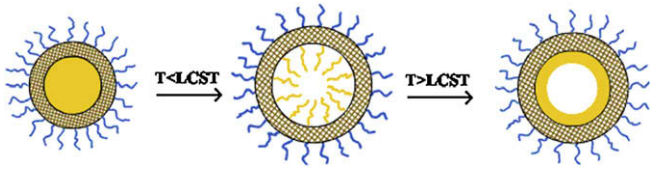

Scheme 2. The swelling and shrinking process of Sample 1.

When the weight ratio of PEG_{114}-*b*-PAA_{156}/$PNIPAM_{53}$-*b*-$P4VP_{109}$ varied from 1/3 to 1/15, the swelling ratios were different and changed from 2.3 to 11.24 (as shown in Table 3). With decreasing the concentration of PEG-*b*-PAA, the number of carboxyls declined, which led to some pyridyls being free from complexation and the resultant shells became looser. The restriction of the shells on the expanding core decreased, so lower degree of cross-linking leaded to a higher swelling ratio. The same trend was also seen in Li's report [35].

In order to fabricate asymmetric hollow particle with a hydrophobic lumen, heating process was carried out again and the change in hydrodynamic diameter is shown in Fig. 9. When the aqueous solution was heated above LCST again, the diameters of the four samples decreased. However, they were still larger than the size at the former 65 °C. Though gel–sol transition happened and PNIPAM became hydrophobic again, it did not shrink back to original solid core since they were not dense enough for the overlapping at a low temperature. As shown in Scheme 2, PNIPAM inside corona which was tethered but stretched and had a relatively low density, showed a non-shrinking behavior at low temperature [36]. When PNIPAM became hydrophobic, the balance between swollen PNIPAM and CLS restriction was broken, which resulted in the shrinkage of the complex shell, so the asymmetric hollow particles became smaller but still larger than the original CSC micelles.

4. Conclusion

Asymmetric hollow particle, with PNIPAM as inside corona, P4VP/PAA complexion as CLS and PEG as corona, was fabricated from adding PEG_{114}-*b*-PAA_{156} aqueous solution into the $PNIPAM_{53}$-*b*-$P4VP_{109}$ micelles aqueous solution at 65 °C followed by PNIPAM block became hydrophilic and swollen when temperature went

down. The asymmetric hollow particle has both hydrophilic PNIPAM inside and PEG outside the shell respectively. The diameter of this asymmetric hollow particle increased from 130.8 to 266.2 nm when the concentration of PEG-*b*-PAA varied from 0.10 to 0.01 mg mL^{-1} while PNIPAM-*b*-P4VP is a constant value of 0.15 mg mL^{-1}. When temperature was above LCST, the PNIPAM would collapse onto the shell and the hydrophilic inside corona transformed into a hydrophobic lumen. The latter asymmetric hollow particle was smaller in size for the shrinkage of the CLS. The cross-linked semipermeable shell and the hydrophobic lumen make this asymmetric hollow particle as an ideal candidate for drug carrier to load hydrophobic drugs. Nevertheless, in this context, clearly more information is needed about the loading and releasing hydrophobic drugs of the asymmetric hollow particles, which is beyond the goal of this paper and, hence, will be reported in the future.

Acknowledgements

The financial support by the National Natural Science Foundation of China (Grant No.: 20774051 and No.: 50830103) and the Outstanding Youth Fund (No. 50625310) is gratefully acknowledged.

References

[1] Yu K, Eisenberg A. Macromolecules 1996;29(19):6359–61.
[2] Zhang LF, Yu K, Eisenberg A. Science 1996;272:1777–9.
[3] Zhang LF, Eisenberg A. Macromolecules 1996;29(27):8805–15.
[4] Luo LB, Eisenberg A. Langmuir 2001;17(22):6804–11.
[5] Choucair A, Lavigueur C, Eisenberg A. Langmuir 2004;20(10):3894–900.
[6] Zhang LF, Eisenberg A. Science 1995;268:1728–31.
[7] Van Hest JCM, Delnoye DAP, Baars MWLP, Van Genderen MHP, Meijer EW. Science 1995;268:1592–5.
[8] Discher DE, Eisenberg A. Science 2002;297:967–73.
[9] Mu MF, Ning FL, Jiang M, Chen DY. Langmuir 2003;19(24):9994–6.
[10] Liu XY, Jiang M, Yang SL, Chen MQ, Chen DY, Yang C, et al. Angew Chem Int Ed 2002;41(16):2950–3.
[11] Dou HJ, Jiang M, Peng HS, Chen DY, Hong Y. Angew Chem Int Ed 2003;42:1516–9.
[12] Weda P, Trzebicka B, Dworak A, Tsvetanov CB. Polymer 2008;49:1467–74.
[13] Koide A, Kishimura A, Osada K, Jang WD, Yamasaki Y, Kataoka K. J Am Chem Soc 2006;128:5988–9.
[14] Nardin C, Hirt T, Leukel J, Meier W. Langmuir 2000;16(3):1035–41.
[15] Stoenescu R, Meier W. Chem Commun 2002;24:3016–7.
[16] Luo LB, Eisenberg A. Angew Chem Int Ed 2002;41:1001–4.
[17] Liu FT, Eisenberg A. J Am Chem Soc 2003;125(49):15059–64.
[18] Ding JF, Liu GJ. J Phys Chem B 1998;102(31):6107–13.
[19] Choucair A, Lim Soo P, Eisenberg A. Langmuir 2005;21(20):9308–13.
[20] Li S, Byrne B, Welsh J, Palmer AF. Biotechnol Prog 2007;23:278–85.
[21] Chen XR, Ding XB, Zheng ZH, Peng YX. New J Chem 2006;30:577–82.
[22] Kishimura A, Koide A, Osada K, Yamasaki Y, Kataoka K. Angew Chem Int Ed 2007;46:6085–8.
[23] Napoli A, Boerakker MJ, Tirelli N, Nolte RJM, Sommerdijk NAJM, Hubbell JA. Langmuir 2004;20(9):3487–91.
[24] Xia JH, Zhang X, Matyjaszewski K. Macromolecules 1999;32(10):3531–3.
[25] Ciampolini M, Nardi N. Inorg Chem 1966;5:41–4.
[26] Xiong DA, Shi LQ, Jiang XW, An YL, Chen X, Lu J. Macromol Rapid Commun 2007;28(2):194–9.
[27] Zhang WQ, Shi LQ, Gao LC, An YL, Li GY, Wu K, et al. Macromolecules 2005;38(3):899–903.
[28] Wu C, Zhou SQ. Macromolecules 1995;28(24):8381–7.
[29] Gao JP, Wei YH, Li BY, Han YC. Polymer 2008;49(9):2354–61.
[30] Tu YF, Wan XH, Zhang D, Zhou QF, Wu C. J Am Chem Soc 2000;122(41):10201–5.
[31] Yang M, Wang W, Yuan F, Zhang XW, Li JY, Liang FX, et al. J Am Chem Soc 2005;27(43):15107–11.
[32] Wilson DL, Kump KS, Eppell SJ, Marchant RE. Langmuir 1995;11(1):265–72.
[33] Yuan XF, Jiang M, Zhao HY, Wang M, Zhao Y, Wu C. Langmuir 2001;17(20):6122–6.
[34] Voets IK, Keizer Ade, Waard Pde, Frederik PM, Bomans PHH, Schmalz H, et al. Angew Chem Int Ed 2006;45:6673–6.
[35] Li YT, Lokitz BS, McCormick CL. Macromolecules 2006;39(1):81–9.
[36] Zhang WA, Zhou XC, Li H, Fang YE, Zhang GZ. Macromolecules 2005;38(3):909–14.